VORTEX BASED METHOD OF FUNDAMENTAL SOLUTIONS FOR AIRFOIL AND BLADE CASCADE FLOW COMPUTATIONS

Fernanda S. Lima[1], **fernandasirio@gmail.com**
Nelson Manzanares-Filho[1], **nelson@unifei.edu.br**
Waldir de Oliveira[1], **waldir@unifei.edu.br**

[1]Universidade Federal de Itajubá – UNIFEI, Minas Gerais, Brasil

Abstract. *The Method of Fundamental Solutions (MFS) is currently a popular boundary-type meshless method that has been applied to solve various engineering problems. In aerodynamic problems involving slender bodies the MFS has been scarcely applied. In this case the outside domain is interior to the bodies and so it is difficult or even impossible to distribute the FS locations adequately. Boundary mesh-based methods experiment excessive numerical errors and convergence difficulties for treating very slender body shapes. For plane aerodynamic problems, auxiliary conformal mappings may help to overcome or to alleviate these drawbacks. For potential incompressible flow problems, the Laplace equation must be satisfied by both the potential function and the stream function. The logarithmic fundamental solution corresponds to the potential induced by a source in the first case and to the stream function induced by a vortex in the second one. In this work, only point vortices are employed in order to represent both isolated and cascade bodies. For airfoils with cusped trailing edges, a conformal mapping is firstly applied in order to transform a profile in the physical plane in a near-circle. The vortex-based MFS is then applied in the near-circle plane. The Joukowski mapping is used for isolated airfoils and the Weinig mapping for blade cascades. Depending on the parameters of these transformations, the obtained near-circles may exhibit excessive curvature variation by impairing the accuracy of the numerical results. To deal with this situation, a suitable technique was developed for producing near-circles with a minimum of curvature variation. For smooth bodies, like circles or thick ellipses, the vortex-based MFS can be applied directly in the physical plane. Various tests were carried out on isolated circles, ellipses, airfoils and blade cascades in order to verify the influence of the number of vortices, their distance from the boundary and also the curvature variation. We concluded that the vortex-based MFS can attain a high degree of accuracy and hence can be used to generate benchmarks for airfoil and cascade flow analysis. With suitable adaptations and extensions the MFS can also be used in the development of reliable tools for turbomachinery blade design.*

Keywords*: Vortex-based Method of Fundamental Solutions, Conformal mapping, Airfoils, Blade Cascade*

1. INTRODUCTION

For a long time the finite element method and the finite difference method have been the dominant numerical methods. These methods are domain-type methods in contrast to boundary-type methods which transfers the problem to the boundary. In general, the domain-type methods require domains meshing and it becomes extremely hard when they are solving 3D problems. Thereby the boundary element methods (BEM) have arisen as alternative techniques that discretize just the boundary which requires low computational cost. However the BEM involves sophisticated mathematics and there are some difficult numerical integrations. Thus meshless methods were developed which require neither domain nor boundary meshing. They need just discretizations via sets of nodes. Related to these methods, the method of fundamental solutions (MFS) has emerged as an effective boundary-only meshless method for solving homogeneous linear partial differential equations. MFS just requires the satisfaction of boundary conditions and the fundamental solutions have to be known.

The idea of the MFS is to approximate the solution by linear combining of the fundamental solutions of the governing differential operator in such a way that the additional boundary conditions are satisfied with sufficient accuracy. It reduces the problem to an interpolation problem on the boundary by fitting the data on the boundary. Another advantage is that the integration domain can be moved outside the domain that contains the singularities, to avoid them. In many cases the total error is bounded by the error on the boundary, which can be evaluated easily. Furthermore, adaptive versions are possible, introducing more trial functions to handle places where the boundary errors are not acceptable. For smooth problems the MFS shows a very good convergence behavior.

One of the first MFS applications was on potential problems, like the study of how the boundary conditions of an elliptic equation can be approximate by FS (Mathon and Johnston, 1977). The FS are used as interpolation functions and the singularities are located outside the domain and its locations let free to change. Therefore a highly adaptive method though nonlinear is found which showed to work well in 3D problems and with boundaries of low continuity class. After some time, the MFS was applied for solving potential flow problems. Dragos (1982) has used this method to determine the FS on the steady linear aerodynamic context and how to use this solution in order to derive the motion in the presence of bodies. Johnston and Fairweather (1984) have used the MFS to obtain the velocity field of a fluid flowing past a cylinder between two parallel plates. The authors show the method advantages which are highly adaptive, the ease to determine the solution by a direct evaluation process and a very good accuracy. Karageorghis and

Fairweather (1999) have studied the application of the MFS to axisymmetric potential problems when it has simple FS (when the boundary conditions and the domain are both axisymmetric) and it has arbitrary boundary conditions. It was showed that the MFS can be applied to any problem that has known FS and the method is very efficient for nonlinear problems.

In this work we applied the MFS to solve a potential fluid flow over a body using vortex points as the singularities (FS). This flow was represented by the Laplace's equation of the stream function. An inverse Joukowski mapping was used to obtain a near-circle and then all the calculations were made in the transformed plane. Some examples are presented in this work, including circles, ellipses, symmetrical and cambered airfoils.

2. MFS BASIC FORMULATION IN THE AERODYNAMIC CONTEXT

As said before, the basic idea of the MFS is to approximate the solution of a homogeneous linear boundary value problem in terms of a superposition of fundamental solutions of the governing differential operator, L. In other words, the fundamental solution $G(x, y)$ is a solution of the homogeneous partial differential equation

$$Lu = 0 \text{ in } \Omega \tag{1}$$

for all domains Ω which do not contain the singular point y of $G(x, y)$. If $\Omega \subset R^d$, $d = 2, 3$, is a bounded open nonempty connected domain with sufficiently regular boundary $\partial\Omega = \Gamma$ and f^Γ is a known function, then the additional boundary condition

$$u = f^\Gamma \text{ on } \Gamma \tag{2}$$

defines together with (1) a homogeneous Dirichlet boundary value problem. It can be express in terms of Neumann boundary value problem

$$\frac{\partial u}{\partial n} = 0 \text{ on } \Gamma, \tag{3}$$

where n is a outer unit normal vector.

In the aerodynamic context, the aim of using this method is to solve a potential flow over a body which can be represented by the velocity potential and source points as the singularities in the case of the Neumann problem, or by the stream function and vortex points in the case of the Dirichlet problem. Therefore, equations (1), (2) and (3) can be written as

$$\begin{cases} \nabla^2 \phi = 0 \\ \dfrac{\partial \phi}{\partial n} = 0 \text{ on } \Gamma \end{cases} \tag{4}$$

for Neumann boundary condition, and the fundamental solution is the potential of a source

$$\phi(z) = \frac{1}{2\pi} \ln r\,, \tag{5}$$

or

$$\begin{cases} \nabla^2 \psi = 0 \\ \psi = cte \text{ on } \Gamma \end{cases} \tag{6}$$

for Dirichlet boundary condition, and the fundamental solution is the stream function of a vortex

$$\psi(z) = -\frac{1}{2\pi} \ln r\,, \tag{7}$$

where z is the location of the singular points in complex coordinates and r is the distance between the collocation and the singular point. We have chosen to use complex variables because of the ease of implementation and computing, but it is also possible to work without a complex formulation.

3. INVERSE CONFORMAL MAPPING FOR AIRFOILS AND BLADE CASCADES

In the case of airfoils it is very difficult to locate the singularities inside the trailing edge region. To avoid that

drawback which limits the use of the MFS, one opted to use an inverse conformal mapping.

For isolated airfoils/bodies the Joukowski mapping was chosen. The Weinig mapping was chosen for blade cascades. The Joukowski mapping is given by

$$z(\zeta) = \zeta + \frac{c^2}{\zeta} \ , \tag{8}$$

where z is the coordinate of a point in the physical plane, ζ is the coordinate in the transformed plane and c is the transformation parameter. An explicit equation was determined for the inverse Joukowski mapping by calculating the roots of Eq. (8) for a given z

$$\zeta(z) = \left(z \pm \sqrt{z^2 - 4c^2}\right) \Big/ 2 \ . \tag{9}$$

One of the roots is inside the circle of radius c and the other is outside it, that is

$$\left|\zeta(z)\right| \geq c \tag{10.a}$$

or

$$\left|\zeta(z)\right| \leq c \ . \tag{10.b}$$

An algorithm was developed for specifying the proper root. Then a near-circle can be obtained for any airfoil with a cusped trailing edge.

As said before, the Weinig mapping was chosen for blade cascades. In this case an inverse mapping was not developed. All the computations were done in the transformed plane. When the circle's center lies on the origin of the coordinates (ξ, η) one has a flat plate cascade. Moving this center by using a parameter μ, one obtains an airfoil cascade. Here the center of the circle was moved only in the ξ direction resulting in a symmetric profile cascade. So the complex potential based on a flat plate cascade is

$$F(\zeta) = \frac{U_\infty t}{2\pi}\left(\ln\frac{\zeta + R}{\zeta - R} + \ln\frac{\zeta + 1/R}{\zeta - 1/R}\right), \tag{11}$$

where t denotes the blade spacing, U_∞ is the incident velocity, R is the location of the singularities that represents the flow at $\pm\infty$ in the physical plane, and $1/R$ is the location of the singularities reflections inside the transformed body. Considering null incidence, for a given stagger angle β, the mapping function is

$$z = \frac{t}{2\pi}\left(\mathrm{e}^{-\mathrm{i}\beta}\ln\frac{\zeta + R}{\zeta - R} + \mathrm{e}^{\mathrm{i}\beta}\ln\frac{\zeta + 1/R}{\zeta - 1/R}\right). \tag{12}$$

During the tests of this method, we have noted that there was an influence of the variation of the curvature deviation along the body contour in the computing accuracy. For instance, computing the error for an ellipse (without mapping), one has observed that the error has suddenly increased when the singularities were placed beyond the curvature center of the edges. This behavior showed the need to locate the singularities near the boundary when one has a significant variation of the curvature deviation. Thus when an inverse conformal mapping technique is applied it is important to obtain a near-circle in the transformed plane as smooth as possible. To attain this goal, an optimum value of the c parameter is determined in order to minimize the curvature deviation of the near-circle. An optimization routine from IMSL FORTRAN library was used.

4. NUMERICAL FORMULATION AND IMPLEMENTATION

In this work one has chosen to use a static implementation, in other words, the location of the singularities (fictitious boundary) is determined a priori. The number of collocation points (points in the body's boundary) and the singular ones were defined to be equal. The algorithm was implemented in FORTRAN.

The input parameters are the given body's boundary data: coordinates of the collocation points (x, y), the leading edge number *nle*, and total number of points *nn* (even), a distance factor δ between the real and fictitious boundaries (to be defined later), and the angle of attack α and, for cascades, the R and μ values. For airfoils and cascades, the calculations are made in the transformed plane. The number of collocation/singular points N is equal to half of *nn*. The other half is set to be the test points, where the value of the stream function is computed in order to obtain the error.

Once given the body's data a subroutine is called to compute the inverse Joukowski mapping and the minimization of the curvature deviation for isolated bodies. For cascades, the input parameters are given directly in the transformed plane and one can obtain the values in the physical plane using the mapping function. The subroutine DUVMIF from IMSL library was applied to the single variable optimization. In the numerical implementation, the system of equations must be discretized as follow

$$\sum_{j=1}^{N} \alpha_j G(x_i, y_j) = f^{\Gamma}(x_i),\ 1 \le i \le N \ . \tag{13}$$

In the aerodynamic context, equation (13) becomes

$$\sum_{j=1}^{N} \Gamma_j \psi_{ij} - \psi_{\infty i} = \psi_0,\ 1 \le i \le N\ , \tag{14}$$

where Γ is the vortex density distribution, $\psi_{i,j}$ is the stream function induced by the singularity j on the collocation point i, $\psi_{\infty,i}$ is the stream function induced by the uniform velocity on the collocation point i, and the ψ_0 is the constant value of the stream function on the boundary (boundary condition). The $\psi_{\infty,i}$ was decomposed in two parts based on α

$$\sum_{j=1}^{N} \Gamma_j \psi_{ij} = x_i \sin(\alpha) - y_i \cos(\alpha) + \psi_0,\ 1 \le i \le N\ . \tag{15}$$

Hence the solution is computed through the superposition of three linear systems derived from equation (15)

$$\sum_{j=1}^{N} \Gamma_j^{0^\circ} \psi_{ij} = -y, \text{ for } U_\infty = 1,\ \alpha = 0^\circ, \text{ and } \psi_0 = 0\ , \tag{16}$$

$$\sum_{j=1}^{N} \Gamma_j^{90^\circ} \psi_{ij} = x, \text{ for } U_\infty = 1,\ \alpha = 90^\circ, \text{ and } \psi_0 = 0\ , \tag{17}$$

$$\sum_{j=1}^{N} \Gamma_j^{\psi_0} \psi_{ij} = 1, \text{ for } U_\infty = 0, \text{ and } \psi_0 = 1\ , \tag{18}$$

where U_∞ is the uniform incident velocity. A LU factoring technique was applied using the IMSL subroutine DLFCRG, which also computes the condition number, and the factoring system was solved using the subroutine DLFSRG. After that the Kutta condition is imposed by taking the resulting tangential velocity on the trailing edge equal to zero. Thus one determine the constant value of the stream function on the collocation points, and Γ is computed by

$$\Gamma_j = \cos(\alpha)\Gamma_j^{0^\circ} + \sin(\alpha)\Gamma_j^{90^\circ} + \psi_0 \Gamma_j^{\psi_0},\ 1 \le j \le N\ . \tag{19}$$

The velocities on the collocation points and the stream function value on the tests points are computed. Then the mean square error, the local error, and the maximum error are determined at the end of the algorithm.

5. EXAMPLES

The proposed method was tested for some bodies in order to analyze its behavior and performance. Different distance factors δ were used. The first chosen example was a circular cylinder. Here δ was defined as a ratio between the fictitious boundary radius and the body's boundary radius. Figure 1.a shows that the method presents a high accuracy when the fictitious boundary moves away from the body's boundary or the number of points N increases.

An unstable region appears when the singular points are located far away and the number of points increases. As the number of points grows for some δ, the condition number raises quickly causing uncertainty in the error accuracy. Figure 1.b shows the possibility of collapsing the curves in order to obtain a reference to chose appropriate parameters for a given accuracy.

Figure 2 shows that the Kutta condition must be applied in order to guarantee a stagnation point at the trailing edge even in the case of null incidence. Otherwise a symmetry loss is observed by creating a false numerical circulation.

Figure 3 shows that the local error distribution gets unstable as the singular points are moved away from the body's boundary.

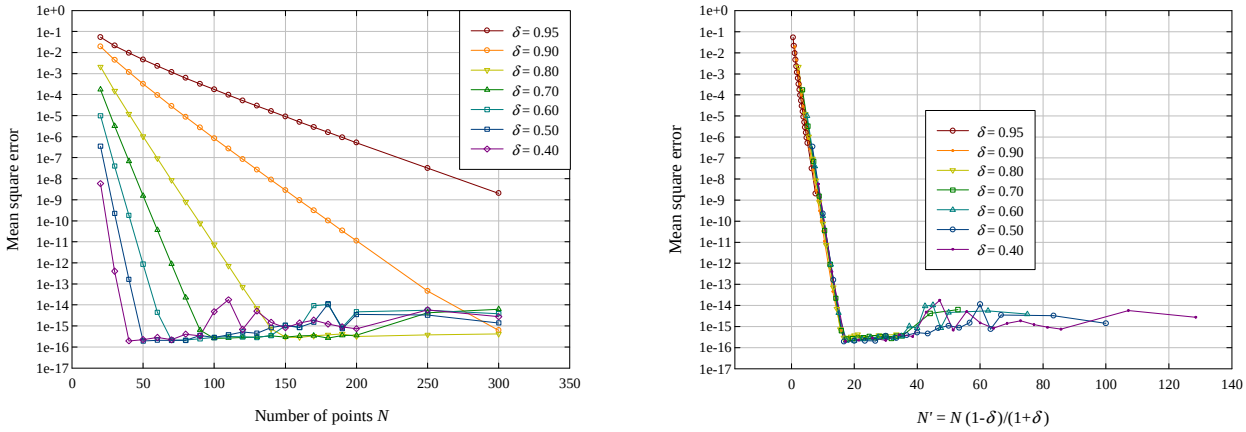

a. b.

Figure 1. Mean square error for the circular cylinder with Kutta condition.

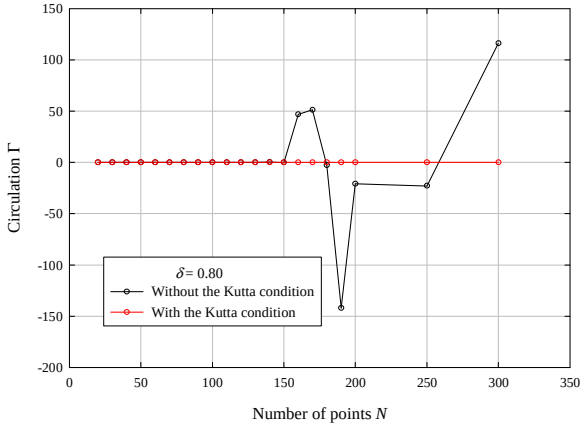

Figure 2. Circulation behavior with and without Kutta condition for $\delta = 0.8$.

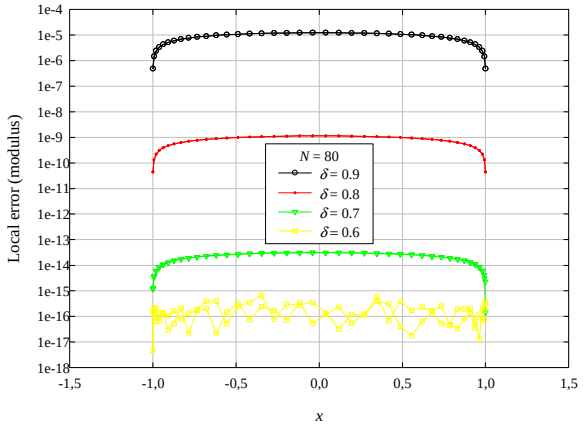

Figure 3. Influence of the δ in the local error distribution.

The second body studied was an ellipse. During the tests it was noted that the results always diverged when the singular points were located beyond the curvature center of the edges. This fact indicates that the curvature variation of the boundary has strong influence in the accuracy. So the distance allowed to locate the singular points was limited to the curvature radius of the edges. Thus δ was defined as the ratio of the distance from the singular point close to the leading edge to the curvature center and the curvature radius. Figures 4.a and 4.b show a convergence behavior similar to the circular cylinder case.

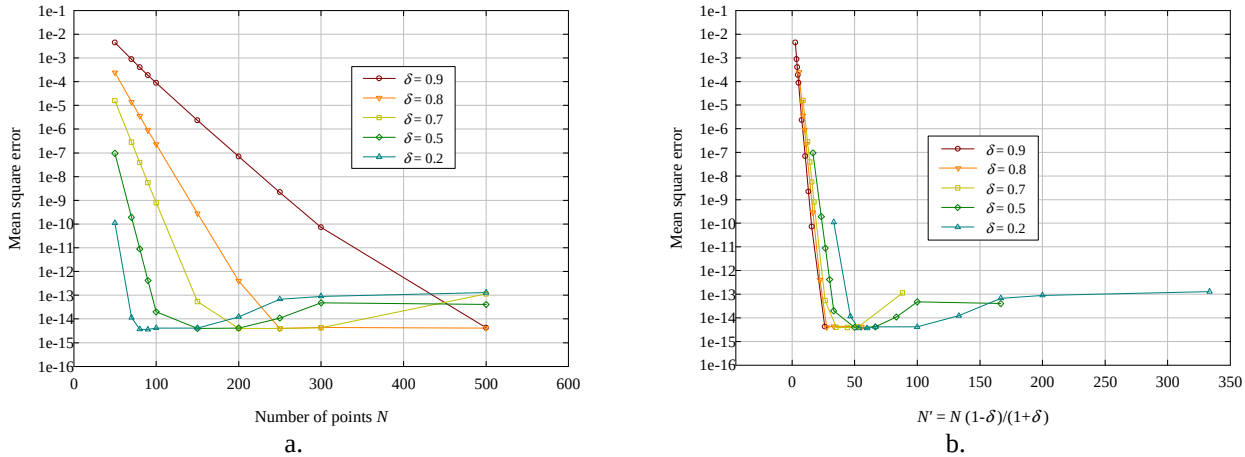

a. b.

Figure 4. Method behavior for an ellipse with aspect ratio 0.5 in the physical plane.

Three airfoil profiles under null incidence were also chosen for testing the developed method: one symmetric airfoil (NACA 65-010) and two cambered airfoils (NACA 65-906 and 65-910). The inverse Joukowski mapping and the procedure for minimization of the curvature deviation were applied (Section 3).

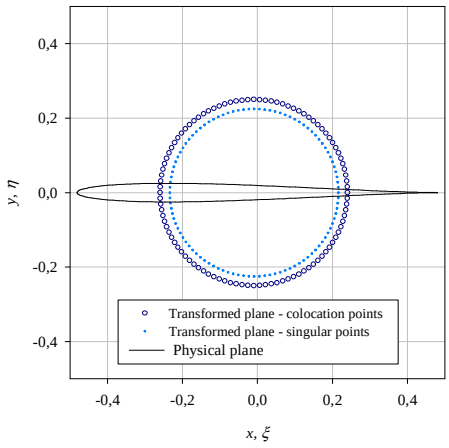

Figure 5. NACA 65-010 profile and its near-circle.

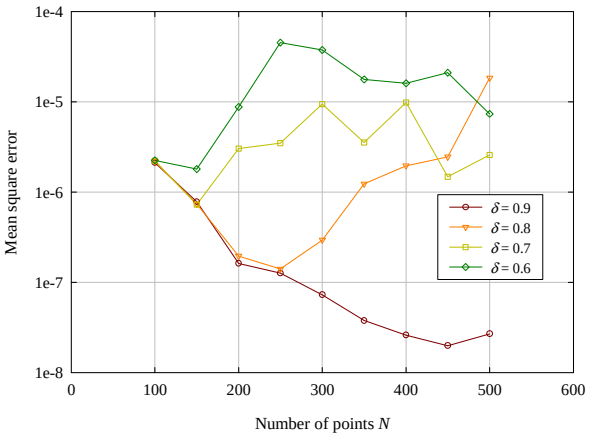

Figure 6. Mean square error for NACA 65-010.

Figure 5 shows the NACA 65-010 in the physical and transformed plane. The results obtained for this case are illustrated in Fig. 6. We can notice the high influence of the curvature variation in the accuracy as the distance of the singular points from the boundary increases. In this case, we should keep the singular points next to the body's boundary and just change the number of points to achieve the required accuracy. For this profile, δ was not limited to the smallest curvature radius found on the boundary of the near-circle. Here δ has the same definition of the circular cylinder example.

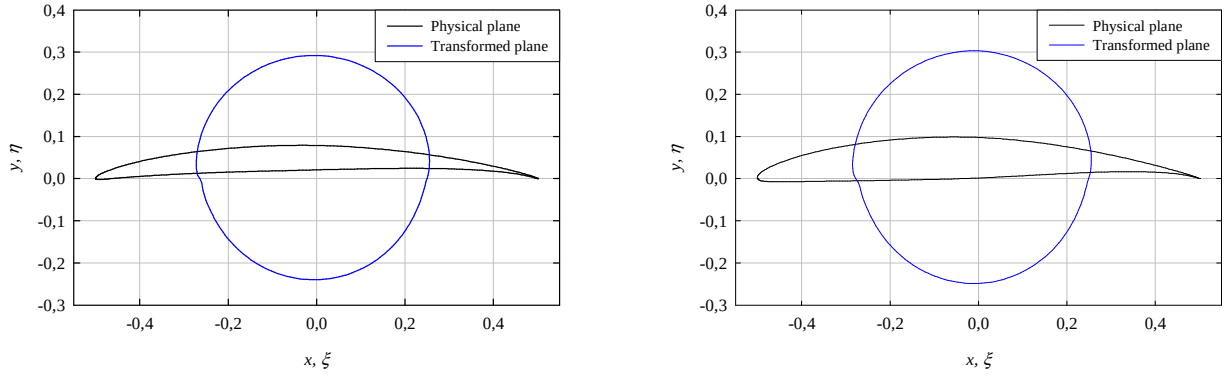

a. b.

Figure 7. a) NACA 65-906 profile and its near-circle. b) NACA 65-910 profile and its near-circle.

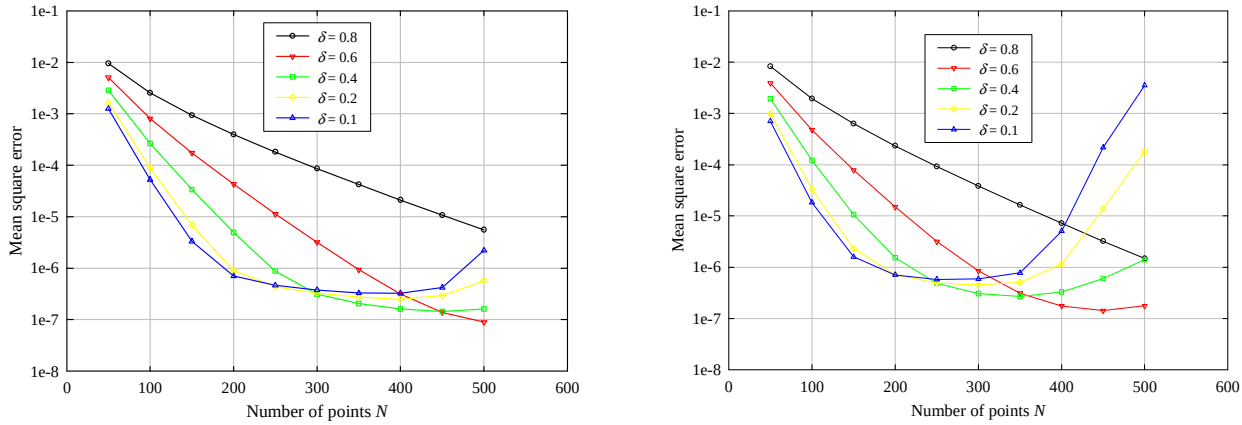

a. b.

Figure 8. Mean square error a)NACA 65-906. b) NACA 65-910.

Figures 7.a and 7.b show the geometry of the cambered airfoils and their corresponding near-circles. The minimization of the curvature deviation was also applied. Now the parameter δ was defined as the ratio of the distance from the singular point close to the convex point of maximum curvature to its curvature center and the minimum curvature radius. Again, we can observe in Figures 8.a and 8.b that the accuracy gets worse as the distance from the boundary increases at high number of points. It is worth mentioning that the airfoil thickness has exerted a significant influence. The equation system becomes more ill-conditioned as the airfoil thickness increases. One observes that the thicker airfoil (Fig. 7.b) attains a minimum error for a lower number of points than the thinner airfoil (Fig. 7.a).

The proposed method was also applied for a flat plate cascade and a symmetric airfoil cascade using the Weinig mapping. One adopted the blade spacing t equal to 1 and null stagger angle β. Since an inverse mapping is not used, the transformed body is a circular cylinder, thus δ is define as the ratio between the fictitious boundary radius and the body's boundary radius. The incident flow was represented by singularities and their reflections inside the transformed body, ensuring that the body´s boundary is part of a stream line (circle theorem). One used R=1,2 and R=2,0 for singularities location.

Figure 9 shows high accuracy of the computation, as expected, in the case of a flat plate cascade. Here, the incident flow was represented only by a source at upstream and a sink at downstream of the body and their reflections inside the body.

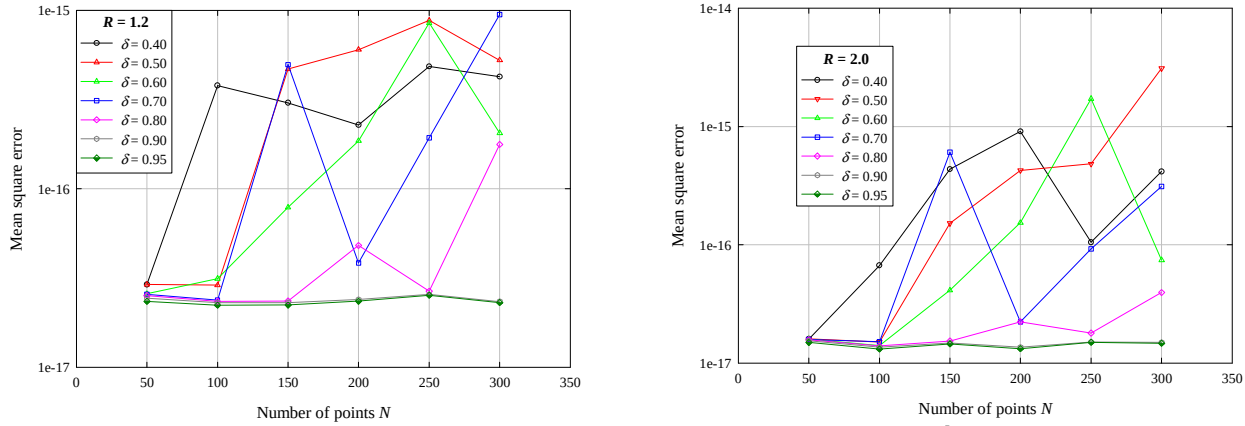

Figure 9. Method behavior using sources and their reflections a) R=1,2. b) R=2,0

Now the incident flow is represented only by a counterclockwise vortex at upstream and a clockwise vortex at downstream of the body and their reflections inside the body. Figure 10 shows a strong influence on accuracy of the computation, impairing the results when one compares to that for the previous case. This behavior shows that a singularities combination of the MFS might helps to solve the equation system better.

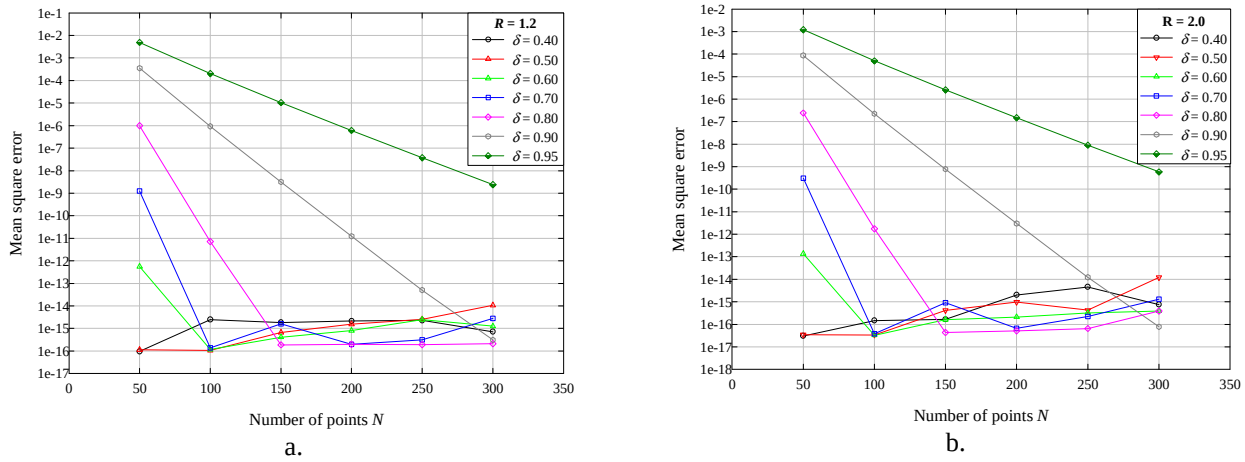

Figure 10. Method behavior using vortices and their reflections a) R=1,2. b) R=2,0

Finally the incident flow is represented by a counterclockwise vortex and a source at upstream and a clockwise vortex and a sink at downstream of the body and their reflections inside the body f. Figure 11 shows a similar behavior of the proposed method to the case of only vortices representing the incident flow.

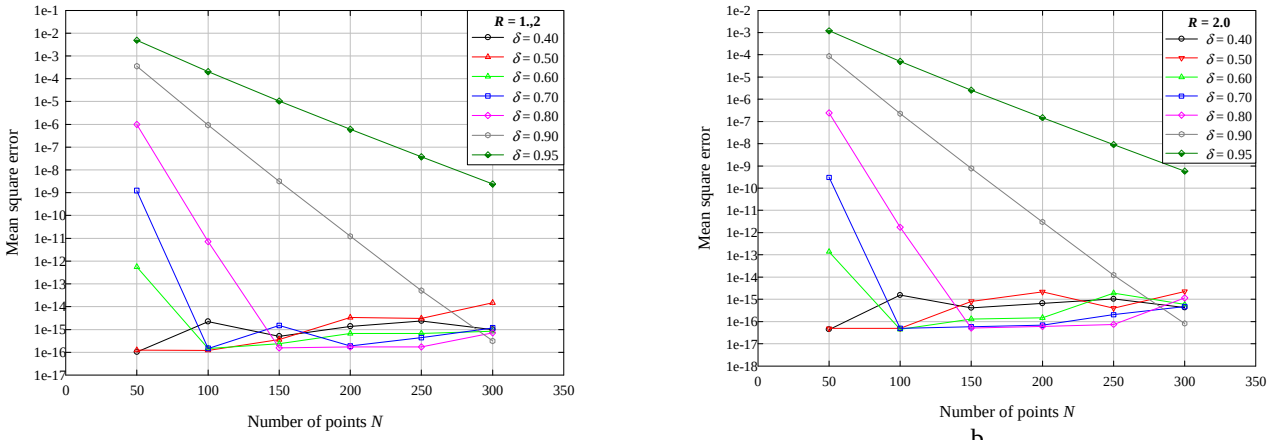

Figure 11. Method behavior using vortices, sources and their reflections a) R=1,2. b) R=2,0

In the case of symmetric airfoil cascade, the transformed body was moved in ξ direction doing μ = -0,05. The symmetric profile obtained in physical plane is shown in Fig. 12.

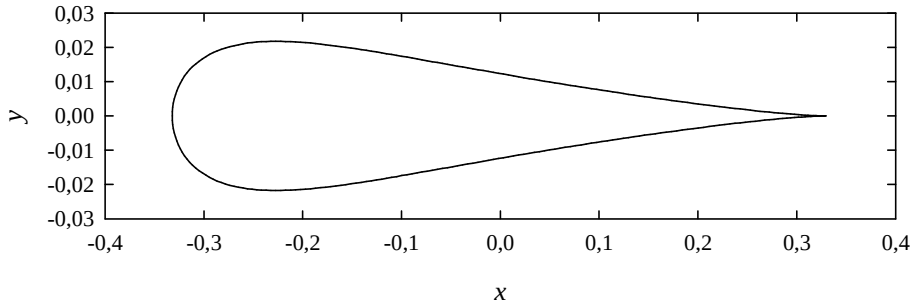

Figure 12. Symmetric profile in physical plane for μ = 0,05.

Figure 13 shows that the error gets worse for the symmetric airfoil cascade. The singularities of the incident flow and the profile thickness had a strong influence on the accuracy of the calculus. Nevertheless one still can obtain a good precision choosing appropriate values for number of points and δ.

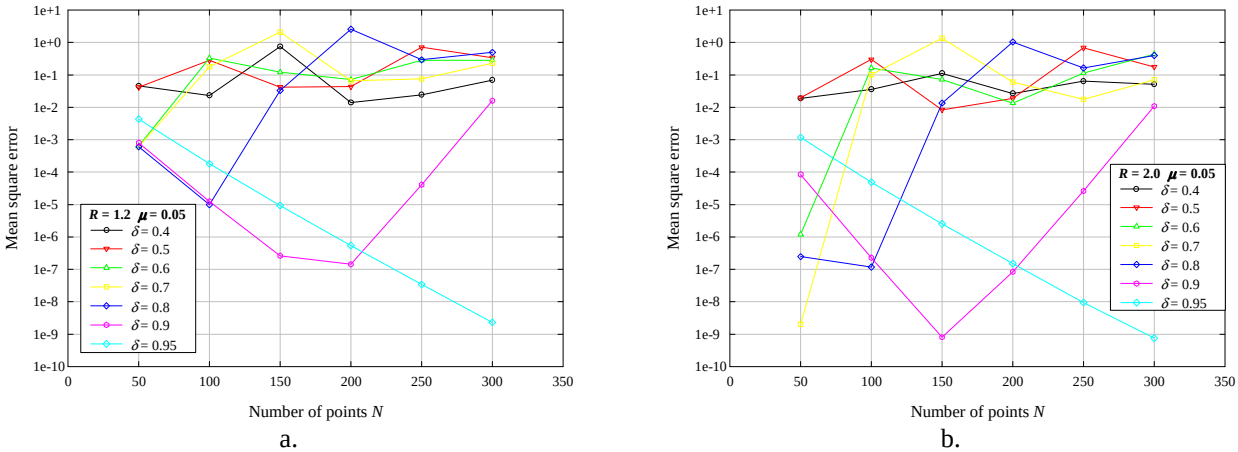

Figure 13. Method behavior using vortices and sources and their reflections for μ = -0,05a) R=1,2. b) R=2,0.

6. CONCLUSIONS

In this work we presented a technique to apply the MFS for solving potential fluid flows over bodies and blade cascades. An inverse conformal mapping was proposed for isolated airfoils to eliminate the difficulty of locating the singularities inside the trailing edge region. A minimization of the curvature deviation was applied to the near-circle to smooth its boundary, improving the accuracy. For cascades, the computations were done directly in the transformed plane. The Vortex-Based MFS showed to be easy to implement and did not require many collocation points and singularities to produce accurate results. Furthermore this method does not involve costly integrations of the boundary, only an evaluation of the approximate solution. The numerical results demonstrate that the proposed method is a powerful method but it showed to be very sensitive to the curvature variations of the body's boundary. The more curvature variation the boundary has, the more uncertain the results are. For cascades, the representation of the incident flow by singularities and profile thickness had also influenced the accuracy.

In future studies, one can combined different kinds of singularities, such as a doublet in the center of the near-circle with vortex points uniformly distributed to improve the results. In addiction one can combine vortices and sources as singularities of the MFS aiming to improve the precision for blade cascades.

7. ACKNOWLEDGEMENTS

This work was developed with financial support of PETROBRAS-CENPES, grant 0050.0034975.07.4 and the CAPES Brazilian agency under PROCAD program.

8. REFERENCES

Chen, C. S., Hon, Y. C., Schaback, R. A., 2008. "Scientific Computing with Radial Basis Functions".

Dragos, L., 1982. "Method of Fundamental Solutions in Plane Steady Linear Aerodynamics". Acta Mechanica 47, pp. 277-282.

Johnston, R. L., Fairweather, G., 1984. "The Method of Fundamental Solutions for Problems in Potential Flow". Applied Mathematical Modeling, vol. 8, pp. 265-270.

Karageorghis, A., Fairweather, G., 1999. "Method of Fundamental Solutions for Axisymmetric Potential Problems". International Journal for Numerical Methods in Engineering 44, pp. 1653-1669.

Karamcheti, K., 1980. "Principles of Ideal-Fluid Aerodynamics". Robert E. Krieger Publishing Company, Malabar, Florida.

Lakshminarayana, B., 1996, "Fluid Dynamics and Heat Transfer of Turbomachinery". John Wiley and Sons Inc., 848 p.

Mathon, R., Johnston, R. L., 1977. "The Approximate Solution of Elliptic Boundary-Value Problems by Fundamental Solutions". SIAM Journal of Numerical Analysis, vol. 14, n. 4, pp. 638-650.

9. RESPONSIBILITY NOTICE

The authors are the only responsible for the printed material included in this paper.